ISSN 0020-1685, Inorganic Materials, 2016, Vol. 52, No. 5, pp. 441–446. © Pleiades Publishing, Ltd., 2016.
Original Russian Text © S.I. Sadovnikov, A.I. Gusev, E.Yu. Gerasimov, A.A. Rempel, 2016, published in Neorganicheskie Materialy, 2016, Vol. 52, No. 5, pp. 487–492.

Silver Sulfide Nanoparticles with a Carbon-Containing Shell

S. I. Sadovnikov[a], A. I. Gusev[a], E. Yu. Gerasimov[b], and A. A. Rempel[a,c]

[a] *Institute of Solid State Chemistry, Ural Branch, Russian Academy of Sciences, Pervomaiskaya ul. 91, Yekaterinburg, 620990 Russia*

[b] *Boreskov Institute of Catalysis, Siberian Branch, Russian Academy of Sciences, pr. Akademika Lavrent'eva 5, Novosibirsk, 630090 Russia*

[c] *Yeltsin Federal University, ul. Mira 19, Yekaterinburg, 620002 Russia*

e-mail: sadovnikov@ihim.uran.ru, gusev@ihim.uran.ru

Received July 22, 2015

Abstract—Silver sulfide nanoparticles have been synthesized through chemical deposition from aqueous solutions of silver nitrate and sodium sulfide in the presence of sodium citrate as a complexing agent and stabilizer. The nanoparticles have a Ag_2S core with a monoclinic crystal structure, covered with a carbon-containing citrate shell. Varying initial reactant concentrations, we can obtain core/shell nanoparticles with a tailored Ag_2S core size and carbon-containing shell thickness.

Keywords: silver sulfide, core–shell nanoparticles, hydrochemical deposition, carbon-containing shell

DOI: 10.1134/S0020168516050149

INTRODUCTION

Reducing the size of structural elements (particles or crystallites) to below some threshold may markedly change the properties of solid substances. In semiconductor nanostructures based on zinc, gallium, cadmium, lead, and silver sulfides, quantum size effects are distinctly observed when the particle size is less than the exciton radius [1, 2]. The size of such particles ranges from 2 to 10 nm and they contain 10^3 to 10^5 atoms. The stability of nanoparticles is ensured by organic ligands chemically bonded to their surface. Nanostructured silver sulfide, Ag_2S, can be used in photochemical cells [3, 4], infrared detectors [5], and solar cells [6]. Isolated stable Ag_2S quantum dots are potentially attractive for use as biological labels [7].

In recent years, a great deal of attention has been paid to the preparation of various core/shell hybrid heteronanostructures: PbS/S, Fe_3O_4/SiO_2, Ag/SiO_2, CdTe/CdSe, and others [8–10]. The core and shell of such particles typically consist of different materials. Particularly widespread are core/shell nanostructures formed by two different semiconductors (GaAs/AlS, CdSe/ZnS, CdSe/CdTe, CdS/Ag_2S, and others). Interest in core/shell particles is also motivated by the necessity of attaching specific groups (organic ligands) to surfaces in order to prevent particle agglomeration, growth, and oxidation and ensure the preparation of stable isolated nanoparticles.

One promising method for producing thin-film structures and nanostructured sulfide semiconductor particles with various structures [11–16] is chemical bath deposition or condensation from solution. Sulfurization can be carried out using hydrosulfuric acid (H_2S), sodium thiosulfate ($Na_2S_2O_3$), sodium sulfide (Na_2S), thiocarbonic acid amide and diamide ($CH_3C(S)NH_2$ and N_2H_4CS), and their derivatives. The particle size can be controlled by varying the number of sulfide nuclei at the initial instant of deposition or condensation.

The purpose of this work was to prepare stable isolated silver sulfide nanoparticles with a carbon-containing citrate shell. Such particles can be thought of as Ag_2S/C core/shell nanostructures. No data on the preparation of such nanostructures have been reported in the literature.

EXPERIMENTAL

Silver sulfide (Ag_2S) nanoparticles and nanopowders were synthesized through chemical deposition from an aqueous solution of silver nitrate ($AgNO_3$) and sodium sulfide (Na_2S), containing sodium citrate, $Na_3C_6H_5O_7$ (Na_3Cit), as a complexing agent and stabilizer, or without it. The starting $AgNO_3$, Na_2S, and Na_3Cit solutions had the same concentration: 50 mmol/L.

The $AgNO_3$ and Na_2S concentrations in all of the reaction mixtures intended for the preparation of silver sulfide were 50 and 25 mmol/L, respectively, and the sodium citrate (Na_3Cit) concentration was varied from 5 to 100 mmol/L. The $AgNO_3$ and Na_2S concen-

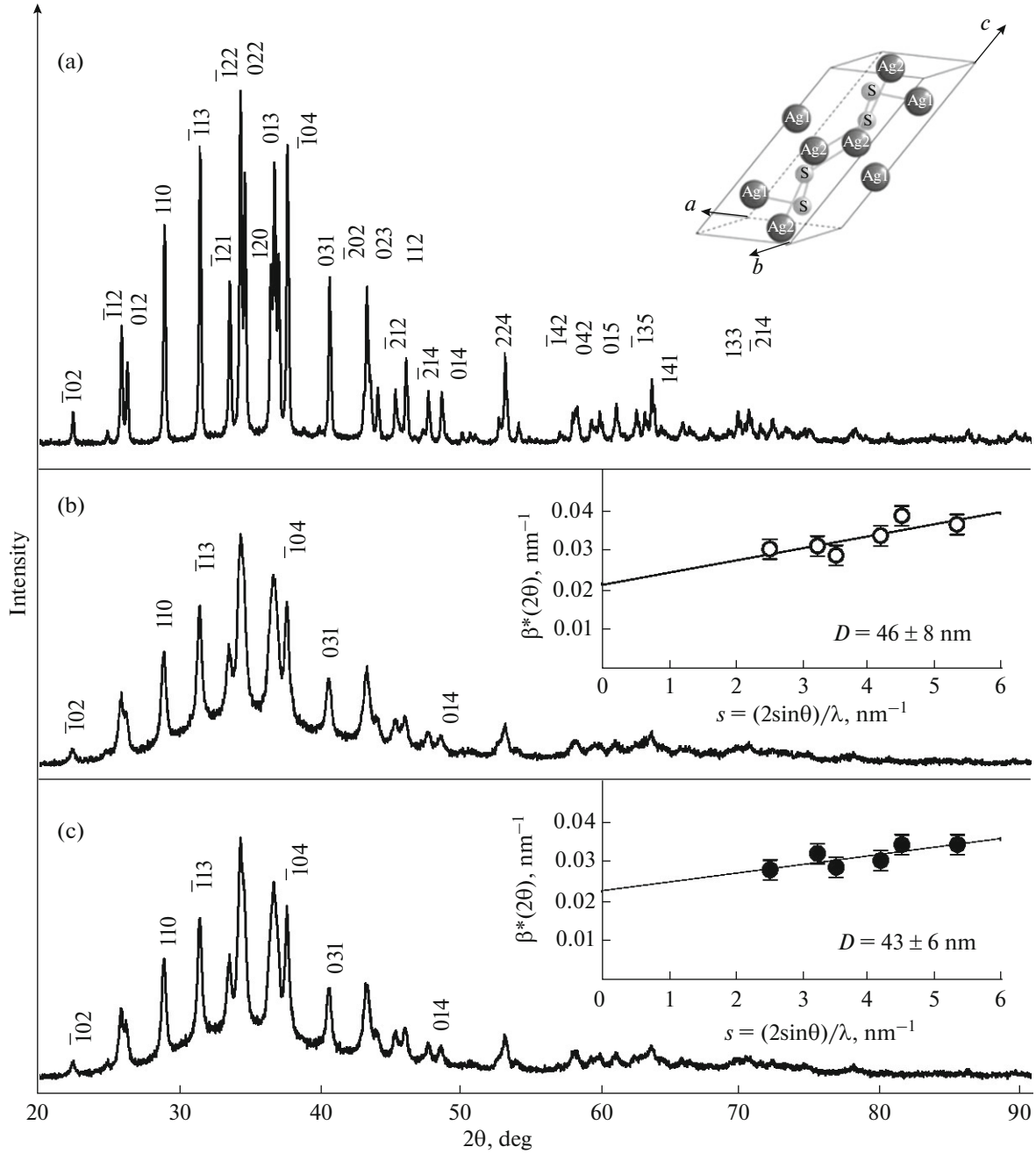

Fig. 1. X-ray diffraction patterns of the synthesized monoclinic (sp. gr. $P2_1/c$) silver sulfide powders: (a) coarse-crystalline powder deposited from the reaction mixture *A*, with $AgNO_3$ and Na_2S concentrations of 50 and 200 mmol/L, respectively; inset: unit cell of acanthite, α-Ag_2S; (b) nanopowder deposited from the reaction mixture *B*, with $AgNO_3$, Na_2S, and Na_3Cit concentrations of concentrations of 50, 25, and 12.5 mmol/L, respectively; (c) nanopowder deposited from the reaction mixture *C*, with $AgNO_3$, Na_2S, and Na_3Cit concentrations of 50, 25, and 25 mmol/L, respectively. The insets in panels b and c illustrate the estimation of the average crystallite size from the broadening of nonoverlapping diffraction peaks.

trations in the reaction mixture containing no complexing agent were 50 and 200 mmol/L, respectively.

All of the deposited powders were characterized by X-ray diffraction on Shimadzu XRD-7000 and STADI-P (STOE) diffractometers ($CuK_{\alpha_{1,2}}$ radiation, angular range $2\theta = 20°–95°$, scan step $\Delta(2\theta) = 0.02°$). To refine the structure of the synthesized Ag_2S powders and determine their lattice parameters, we used the X'Pert Plus software package [17].

The average crystallite size *D* (the average size of coherently scattering domains) of the deposited silver sulfide powders was determined from the broadening

Refined crystal structure of the monoclinic (sp. gr. $P2_1/c$ ($P12_1/c1$)) $Ag_{1.93}S$ nanopowder with the acanthite (α-Ag_2S) structure: a = 0.4234(3) nm, b = 0.6949(3) nm, c = 0.9549(5) nm, β = 125.43(6)°

Atom	Atomic coordinates			Occupancy
	x	y	z	
Ag1	0.0715(4)	0.0151(0)	0.3093(9)	0.97(1)
Ag2	0.7264(3)	0.3240(9)	0.4375(0)	0.96(4)
S	0.4920(2)	0.2339(8)	0.1321(1)	1.00(0)

All positions are 4*e*.

of X-ray diffraction line profiles using the dependence of the reduced broadening of reflections, $\beta^*(2\theta) = [\beta(2\theta)\cos\theta]/\lambda$, on the scattering vector $s = (2\sin\theta)/\lambda$ [1, 14]. The broadening $\beta(2\theta)$ was determined by comparing the observed full width at half maximum, $FWHM_{obs}$, of each diffraction line profile to the instrumental resolution function $FWHM_R$ of the diffractometer.

The size (hydrodynamic diameter D_{DLS}) of the Ag_2S nanoparticles directly in the colloidal solutions was determined by dynamic light scattering (DLS) on a Zetasizer Nano ZS system (Malvern Instruments Ltd) at a temperature of 298 K.

Colloidal silver sulfide nanoparticles were examined by high-resolution transmission electron microscopy (HRTEM) on a JEOL JEM-2010 microscope at a resolution of 0.14 nm. The elemental chemical composition of the Ag_2S nanoparticles was determined by energy dispersive X-ray (EDX) microanalysis on the JEM-2010 using an EDAX Phoenix energy-dispersive spectrometer equipped with a Si(Li) detector (energy resolution, 130 eV). Before HRTEM examination, colloidal solutions of silver sulfide nanoparticles were applied to a copper grid.

RESULTS AND DISCUSSION

The solubility product K_{sp} of silver sulfide (Ag_2S) is very low, 6.3×10^{-50} at a temperature of 298 K [18], and, at a sufficient Na_2S concentration in the reaction mixture, Ag_2S precipitates almost instantaneously, according to the following reaction scheme:

$$2AgNO_3 + Na_2S \xrightarrow{Na_3C_6H_5O_7} \rightarrow Ag_2S\downarrow + 2NaNO_3. \quad (1)$$

After the reactant solutions are poured together, the reaction mixture first blackens. Next, Ag_2S particles precipitate. The largest particles settle down over a period of 1 h. Medium-sized particles (50–80 nm) form agglomerates and also settle down. The precipitation takes about 24 h to reach completion, and the solution becomes transparent. To drive the sulfurization process to completion, the resultant deposit was left in the mother liquor for three days.

The deposited Ag_2S powders were then washed with distilled water and dried in air at a temperature of 323 K. The powders thus obtained were used to determine the crystal structure of the synthesized silver sulfide by X-ray diffraction.

Figure 1 shows X-ray diffraction patterns of the synthesized silver sulfide powders, with different particle sizes. The coarse-crystalline Ag_2S powder represented in Fig. 1a, with a particle size of ≃500 nm, was deposited from the reaction mixture *A*, with no complexing agent. The $AgNO_3$ and Na_2S concentrations in mixture *A* were 50 and 200 mmol/L, respectively. The Ag_2S nanopowder represented in Fig. 1b was deposited from the reaction mixture *B*, in which the $AgNO_3$, Na_2S, and Na_3Cit concentrations were 50, 25, and 12.5 mmol/L, respectively. The nanopowder represented in Fig. 1c was deposited from the reaction mixture *C*, in which the $AgNO_3$ and Na_2S concentrations were the same as in mixture *B*, whereas the Na_3Cit concentration was twice as high: 25 mmol/L. All of the powders have a monoclinic (sp. gr. $P2_1/c$) acanthite (α-Ag_2S) structure. The diffraction peaks of the nanopowders are broadened, so neighboring reflections overlap. The insets at the X-ray diffraction patterns in Figs. 1b and 1c illustrate the estimation of the average crystallite size *D* from the broadening of nonoverlapping diffraction peaks. According to these estimates, the average crystallite size *D* of the Ag_2S nanopowders precipitated from the reaction mixtures *B* and *C* is 46 ± 8 and 43 ± 6 nm. As the sodium citrate concentration increases from 0 to 25 mmol/L, the broadening of the diffraction peaks increases, the particle size of the deposited powders decreases, and the time needed for silver sulfide powder deposition increases.

Structure refinement results for the silver sulfide nanopowders demonstrate that the atomic position coordinates of Ag and S and the unit-cell parameters of the nanopowders are similar to those in macrocrystalline Ag_2S with the acanthite structure. At the same time, the occupancy of the Ag1 and Ag2 silver atoms on the crystallographic position 4*e* in the nanopowders is somewhat lower than unity. A quantitative analysis of X-ray diffraction data and comparison with previous results [19] indicate that the observed set of diffraction peaks corresponds to nanocrystalline nonstoichiometric monoclinic (sp. gr. $P2_1/c$) acanthite α-$Ag_{1.93}S$ (table).

Colloidal solutions over precipitates contain the smallest silver sulfide nanoparticles. After decantation, such solutions remain stable for a year or a longer time, without precipitation. Therefore, the nanoparticles in a colloidal solution are no larger than ≃40 nm in size. These colloidal solutions were used for nanoparticle size determination by DLS and subse-

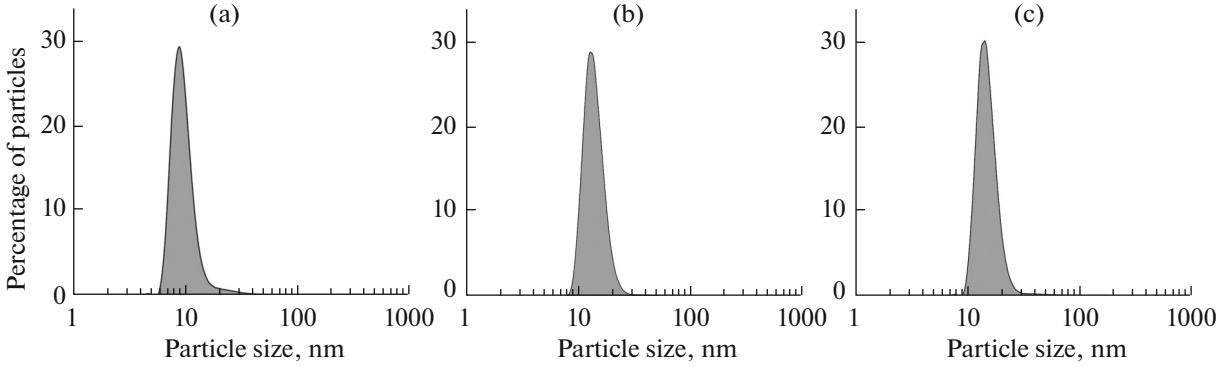

Fig. 2. Size distributions of silver sulfide (Ag_2S) nanoparticles in colloidal solutions: (a) *A*, (b) *B*, (c) *C*.

quent electron-microscopic examination of the colloidal Ag_2S nanoparticles.

DLS measurements showed the following: In the colloidal solution *A*, prepared from the reaction mixture *A*, containing no sodium citrate, the average nanoparticle size is ≃10 nm (Fig. 2a). In the colloidal solution *B*, prepared from the reaction mixture *B*, the average nanoparticle size is about 13 nm (Fig. 2b). In the colloidal solution *C*, prepared from the reaction mixture *C*, the particle size ranges from 9 to 35 nm and the average nanoparticle size is 16 nm (Fig. 2c).

As the sodium citrate concentration increases from 0 to 25 mmol/L, the size of the silver sulfide nanoparticles in the colloidal solutions and the particle size of the precipitated powders vary in opposite ways: the size of the colloidal nanoparticles increases, whereas the particle size of the powders decreases.

Electron-microscopic examination of nanoparticles in the colloidal solutions prepared from the reaction mixtures with different sodium citrate concentrations showed that the solutions contained nanoparticles with and without a shell.

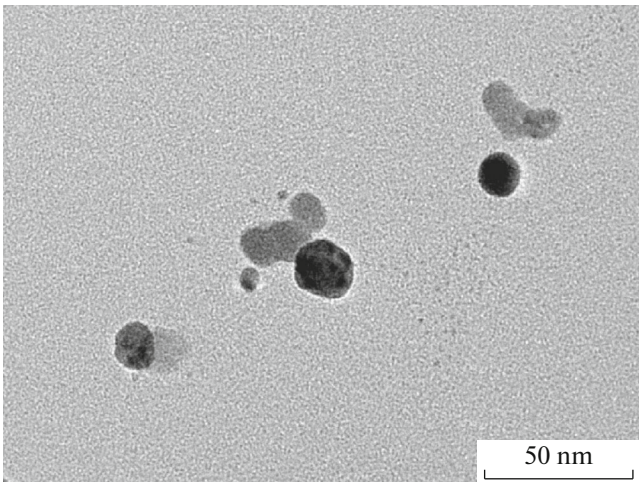

Fig. 3. TEM image of silver sulfide nanoparticles from the colloidal solution *A*.

According to TEM results, the nanoparticles present in the colloidal solution *A*, prepared without sodium citrate (Na_3Cit), had no shell. Most of the nanoparticles were 2 to 8 nm in size (Fig. 3), but there were also larger particles, up to 20 nm in size. This agrees with the above results of DLS measurements (Fig. 2).

HRTEM examination of nanoparticles isolated from the sodium citrate-containing colloidal solutions showed that the sulfide nanoparticles had a shell (Fig. 4). Its thickness was observed to increase with an increase in the time the nanoparticles were kept in the colloidal solution containing the citrate ($C_6H_5O_7^{3-}$) ion (Fig. 4). The observed interplanar spacings in the cores of the hybrid nanoparticles confirmed that the colloidal silver sulfide nanoparticles had a monoclinic structure.

According to EDX analysis data (Fig. 5), the silver and sulfur contents of the core/shell colloidal nanoparticles correspond to a sulfide with the composition $Ag_{1.95-1.98}S$. In addition to silver and sulfur, the EDX spectra of the nanoparticles contain a carbon K_α line, a weak oxygen K_α line, and a copper K_α line, which originated from the copper grid to which the colloidal solutions containing the nanoparticles under investigation were applied. According to the EDX analysis data, the oxygen is distributed over the surface layer of the core/shell nanoparticles. It is reasonable to assume as a first approximation that it is the oxygen of the citrate shell or the oxygen present in adsorbed water. No other elements were detected in the core/shell nanoparticles.

According to the EDX analysis data, the carbon content increases with increasing shell thickness. This means that the shell of the sulfide nanoparticles contains carbon and consists of a citrate.

Indeed, the carboxyl groups of sodium citrate (Na_3Cit) have high affinity for silver ions. This is favorable for the attachment of citrate groups to the

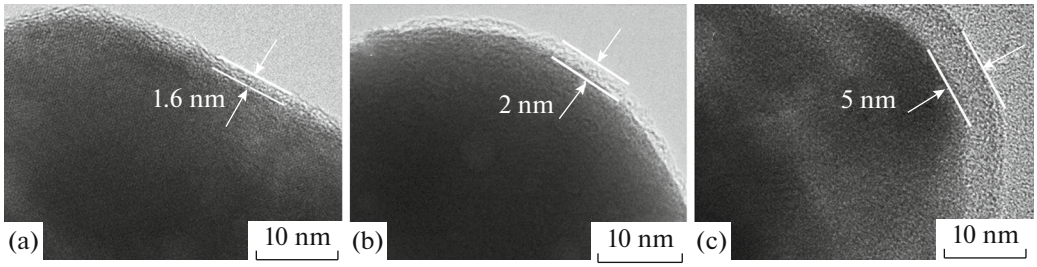

Fig. 4. HRTEM images of colloidal silver sulfide nanoparticles, illustrating the growth of the carbon-containing citrate shell with an increase in the time the nanoparticles are kept in solution: (a) 20, (b) 40, and (c) 1200 min.

surface of silver sulfide nanoparticles and prevents them from agglomerating into large particles. In other words, citrate ions ($C_6H_5O_7^{3-}$) adsorb on the surface of nanoparticles to form a carbon-containing citrate shell, which prevents further growth and agglomeration of the nanoparticles.

The formation of a carbon-containing citrate shell on a silver sulfide (Ag_2S) core occurs as follows: In a sodium citrate-containing solution, $C_6H_5O_7^{3-}$ ions adsorb on the surface of silver sulfide (Ag_2S) nanoparticles and initially form a discontinuous shell nonuniform in thickness. The holes are subsequently filled with citrate complexes until the formation of a continuous carbon-containing shell. The adsorption of citrate complexes by the growing coating makes the shell surface smoother. Increasing the time the nanoparticles are kept in a sodium citrate-containing solution leads to an increase in the thickness of the carbon-containing shell.

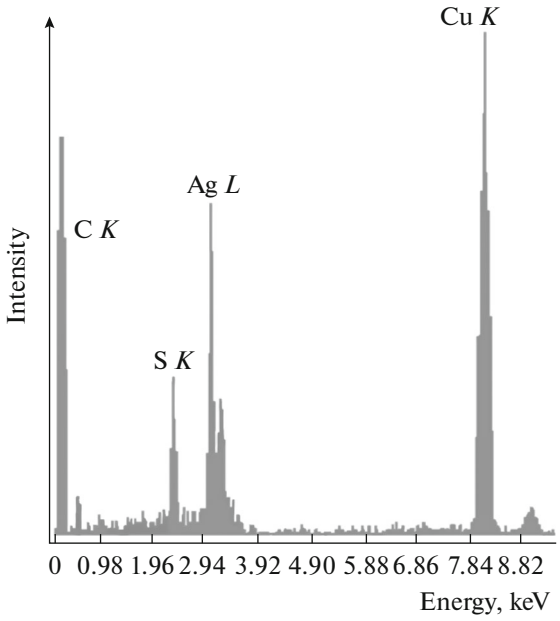

Fig. 5. Elemental EDX analysis of Ag_2S nanoparticles with a carbon-containing citrate shell. The weak oxygen K_α line is observed at 0.525 keV.

CONCLUSIONS

Comparison of the present TEM and X-ray diffraction data indicates the formation of stable, isolated silver sulfide nanoparticles under the deposition conditions used in this study. The nanoparticles have a single-crystal Ag_2S core covered with a continuous carbon-containing shell. Varying initial reactant concentrations and deposition conditions, we can obtain isolated silver sulfide nanoparticles with different Ag_2S core sizes and different carbon-containing citrate shell thicknesses.

ACKNOWLEDGMENTS

This research was supported by the Russian Science Foundation (project no. 14-23-00025) and performed at the Institute of Solid State Chemistry, Ural Branch, Russian Academy of Sciences (Yekaterinburg).

REFERENCES

1. Gusev, A.I. and Rempel, A.A., *Nanocrystalline Materials,* Cambridge: Cambridge Int. Science, 2004.
2. Rempel, A.A., Nanotechnologies, properties, and applications of nanostructured materials, *Usp. Khim.,* 2007, vol. 76, no. 5, pp. 474–500.
3. Lokhande, C.D., Patil, P.S., Yermune, V.S., and Pawar, S.H., Electrodeposition of Ag_2S film from aqueous bath, *Bull. Electrochem.,* 1990, vol. 6, pp. 842–844.
4. Nasrallah, T.B., Dlala, H., Amlouk, M., Belgacem, S., and Bernede, J.C., Some physical investigations on Ag_2S thin films prepared by sequential thermal evaporation, *Synth. Met.,* 2005, vol. 151, no. 3, pp. 225–230.
5. Karashanova, D., Nihtianova, D., Starbova, K., and Starbov, N., Crystalline structure and phase composition of epitaxially grown Ag_2S thin films, *Solid State Ionics,* 2004, vol. 171, nos. 3–4, pp. 269–275.
6. El-Nahass, M.M., Farag, A.A.M., Ibrahim, E.M., and Abd-El-Rahman, S., Structural, optical and electrical

properties of thermally evaporated Ag_2S thin films, *Vacuum,* 2004, vol. 72, no. 4, pp. 453–460.

7. Peng Jiang, Chun-Nan Zhu, Zhi-Ling Zhang, Zhi-Quan Tian, and Dai-Wen Pang, Water-soluble Ag_2S quantum dots for near-infrared fluorescence imaging in vivo, *Biomaterials,* 2012, vol. 33, no. 20, pp. 5130–5135.
8. Lukashin, A.V., Eliseev, A.A., Zhuravleva, N.G., Vertegel, A.A., Tretykov, Yu.D., Lebedev, O.I., and Van Tendeloo, G., One-step synthesis of shelled PbS nanoparticles in a layered double hydroxide matrix, *Mend. Commun.,* 2004, vol. 14, no. 4, pp. 174–176.
9. Vasil'ev, R.B., Vinogradov, V.S., Dorofeev, S.G., Kozyrev, S.P., Kucherenko, I.V., and Novikova, N.N., IR-active vibrational modes of CdTe and CdSe colloidal quantum dots and CdTe/CdSe core/shell nanoparticles and coupling effects, *Phys. Solid State,* 2007, vol. 49, no. 3, pp. 523–526.
10. Hayes, R., Ahmed, A., Edge, T., and Zhang, H., Core–shell particles: preparation, fundamentals and applications in high performance liquid chromatography, *J. Chromatogr., A,* 2014, vol. 1357, pp. 36–52.
11. Lokhande, C.D., Chemical deposition of metal chalcogenide thin films, *Mater. Chem. Phys.,* 1991, vol. 27, no. 1, pp. 1–43.
12. Zhang, W., Zhang, L., Hui, Z., Zhang, X., and Qian, Y., Synthesis of nanocrystalline AgS in aqueous solution, *Solid State Ionics,* 2000, vol. 130, pp. 111–114.
13. Pawar, S.M., Pawar, B.S., Kim, J.H., Joo, O.-S., and Lokhande, C.D., Recent status of chemical bath deposited metal chalcogenide and metal oxide thin films, *Curr. Appl. Phys.,* 2011, vol. 11, pp. 117–161.
14. Sadovnikov, S.I. and Gusev, A.I., Chemical deposition of nanocrystalline lead sulfide powders with controllable particle size, *J. Alloys Compd.,* 2014, vol. 586, pp. 105–112.
15. Sadovnikov, S.I., Gusev, A.I., and Rempel, A.A., Artificial silver sulfide Ag_2S: crystal structure and particle size in deposited powders, *Superlatt. Microstruct.,* 2015, vol. 83, pp. 35–47.
16. Sadovnikov, S.I. and Rempel, A.A., Synthesis of nanocrystalline silver sulfide, *Inorg. Mater.,* 2015, vol. 51, no. 8, pp. 759–766.
17. *X'Pert Plus Version 1.0. Program for Crystallography and Rietveld Analysis,* Amsterdam: Koninklijke Philips Electronics, 1999.
18. Lur'e, Yu.Yu., *Spravochnik po analiticheskoi khimii* (Handbook of Analytical Chemistry), Moscow: Khimiya, 1967, p. 94.
19. Sadovnikov, S.I., Gusev, A.I., and Rempel, A.A., Nonstoichiometry of nanocrystalline monoclinic silver sulfide, *Phys. Chem. Chem. Phys.,* 2015, vol. 17, no. 19, pp. 12 466–12 471.